

AD-A121 161

WATER VAPOR AS A TRACER IN REMOTE WIND SENSING: A
FEASIBILITY STUDY(U) ARMY ELECTRONICS RESEARCH AND
DEVELOPMENT COMMAND WSMR NM ATN. T L BARBER AUG 82
ERADCOM/ASL-TR-0117 F/G 14/2

1/1

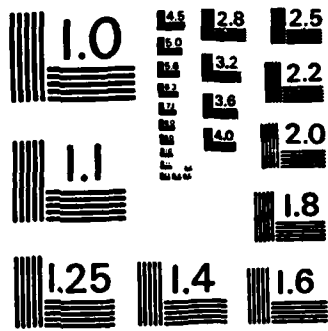
UNCLASSIFIED

NL

END

FORM

010



MICROCOPY RESOLUTION TEST CHART
NATIONAL BUREAU OF STANDARDS - 1963 - A

12



TR-0117

AD

Reports Control Symbol
OSD - 1366

**WATER VAPOR AS A TRACER IN REMOTE WIND SENSING:
A FEASIBILITY STUDY**

AUGUST 1982

By

T. L. Barber

ADA121161

DTIC
ELECTE
NOV 05 1982
S **D**
E

Approved for public release; distribution unlimited.

RE FULL COPY



US Army Electronics Research and Development Command

Atmospheric Sciences Laboratory

White Sands Missile Range, NM 88002

72 05 015

NOTICES

Discrimers

The findings in this report are not to be construed as an official Department of the Army position, unless so designated by other authorized documents.

The citation of trade names and names of manufacturers in this report is not to be construed as official Government indorsement or approval of commercial products or services referenced herein.

Disposition

Destroy this report when it is no longer needed. Do not return it to the originator.

| REPORT DOCUMENTATION PAGE | | READ INSTRUCTIONS BEFORE COMPLETING FORM |
|---|----------------------------------|--|
| 1. REPORT NUMBER ASL-TR-0117 | 2. GOVT ACCESSION NO. A121161 | 3. RECIPIENT'S CATALOG NUMBER |
| 4. TITLE (and Subtitle) WATER VAPOR AS A TRACER IN REMOTE WIND SENSING: A FEASIBILITY STUDY | | 5. TYPE OF REPORT & PERIOD COVERED Final Report |
| | | 6. PERFORMING ORG. REPORT NUMBER |
| 7. AUTHOR(s) T. L. Barber | | 8. CONTRACT OR GRANT NUMBER(s) |
| 9. PERFORMING ORGANIZATION NAME AND ADDRESS US Army Atmospheric Sciences Laboratory White Sands Missile Range, NM, 88002 | | 10. PROGRAM ELEMENT, PROJECT, TASK AREA & WORK UNIT NUMBERS DA Task 1L161102B53A |
| 11. CONTROLLING OFFICE NAME AND ADDRESS US Army Electronics Research and Development Command Adelphi, MD 20783 | | 12. REPORT DATE August 1982 |
| | | 13. NUMBER OF PAGES 27 |
| 14. MONITORING AGENCY NAME & ADDRESS (if different from Controlling Office) | | 15. SECURITY CLASS. (of this report) UNCLASSIFIED |
| | | 15a. DECLASSIFICATION/DOWNGRADING SCHEDULE |
| 16. DISTRIBUTION STATEMENT (of this Report) Approved for public release; distribution unlimited. | | |
| 17. DISTRIBUTION STATEMENT (of the abstract entered in Block 20, if different from Report) | | |
| 18. SUPPLEMENTARY NOTES | | |
| 19. KEY WORDS (Continue on reverse side if necessary and identify by block number) Lidar Remote wind measurement Atmospheric studies | | |
| 20. ABSTRACT (Continue on reverse side if necessary and identify by block number) The military is becoming aware of its need for real-time wind information. The variation in absolute water vapor content can be used as the tracer for a remote wind measurement. This feasibility study is believed to be the first attempt to use a property of water vapor to measure the wind remotely. An example is presented and discussed for a wind measurement at a 500-m range. | | |

CONTENTS

INTRODUCTION..... 5
BACKGROUND..... 5
PROCEDURE..... 7
THEORY..... 11
CALCULATIONS..... 14
DATA ANALYSIS..... 18
CONCLUSIONS..... 21
REFERENCES..... 22

| | |
|--------------------|-------------------------------------|
| Accession For | |
| NTIS GRA&I | <input checked="" type="checkbox"/> |
| DTIC TAB | <input type="checkbox"/> |
| Unannounced | <input type="checkbox"/> |
| Justification | |
| 2 - | |
| Distribution/ | |
| Availability Codes | |
| Dist | Avail and/or Special |
| A | |



INTRODUCTION

The military is becoming aware of its need for real-time remote wind information in various kinds of weather. Wind information of this kind is useful for wind correction of unguided ballistic projectiles for improved first round hit capability.

A high relative humidity condition--all atmospheric water essentially in the vapor phase--is felt to be the meteorological condition in which this specific information is of the greatest value to a military field unit. The method chosen to make the wind measurement must be capable of producing information appropriate for the ballistic correction required. An unguided ballistic device, for best results, requires a crosswind correction measured in the projectile flight path in real-time. Generally, the first few hundred meters is the critical portion of the flight path as relates to ballistic wind correction. Methods are referenced for measuring the wind velocity remotely by using atmospheric dust as a wind tracer.

This paper presents an investigation, however, that is believed to be the first attempt to use water vapor as a remote wind tracer and discusses the theory and feasibility of a remote wind sensing procedure based on measuring the motion of water vapor microstructure by the Differential Absorption Lidar (DIAL) technique. The ordinary Raman backscatter technique is also considered. An example is given for a measurement of the wind at a range of 500 m that appears to be practical for a total measurement time of under 15 s.

BACKGROUND

In the past, wind corrections for unguided ballistic projectiles were taken at a single point with propeller anemometers. Occasionally, pibal (pilot-balloon) observations of wind measurements were used for wind correction above the surface. For long range projectiles, radiosonde wind information was used at higher altitudes. These various measurements lagged badly in time, and the measurement position was poor. The fact that these measurement types are not taken in the path that the projectile will travel is still another disadvantage. A measuring technique that will be far more appropriate for the best correction is one that will give real-time information of the wind profile along the projectile's path. A remote wind measuring method can fulfill these criteria much better than past techniques.

In the past several years, researchers have reported several single ended remote lidar wind measuring techniques in the open literature. Schwiesow and Cupp¹ and Post et al² demonstrated the feasibility of using the Doppler technique, with a continuous wave (cw) CO₂ lidar, for measuring the horizontal

¹Schwiesow, R. L., and R. E. Cupp, "Remote Doppler Velocity Measurements of Atmospheric Dust Devil Varieties," Appl Opt, 15:1, 1976.

²Post, M. J., et al, "A Comparison of Anemometer and Lidar Sensed Wind Velocity Data," J Appl Meteorol, 17:1179-1181, 1978.

wind component parallel to the laser beam. With this specific method, however, the most important component in ballistic wind correction--the wind component perpendicular to the laser beam--cannot be measured.

Teoste and Capes,³ using the Doppler technique with a pulsed CO₂ lidar that conically scans, showed the potential of such a device for producing a vertical wind profile of the horizontal components to an altitude of 8 to 10 km. This approach is limited because it will obtain only the wind profile directly over the device, not the perpendicular wind component across the path of interest. Schotland⁴ developed a Doppler visible light lidar in which an argon laser with a modulated cw beam is used to observe Doppler shifts in the modulation frequency. This approach, too, is limited because it will measure only the velocity vector along the laser beam.

Kunkel et al⁵ and Sroga et al⁶ reported on a technique for measuring wind velocity and direction in a horizontal plane by tracking tenuous natural dust clouds in the atmosphere. Using a scanning lidar, this approach has been demonstrated out to a range of 8 km.

Derr et al⁷ discussed the feasibility of the transit-time lidar (TTL) technique and demonstrated the principle with some pronounced dust irregularities. But these techniques appeared to be slow because they depend upon observing the scattering patterns from the dust in two specific volumes. Armstrong et al⁸ and Barber et al⁹ examined the TTL method as a wind measuring technique for accuracy in an enhanced dust condition. Performed at a range of 250 m, this research discussed sample rates and volume spacings as well. The TTL method does produce the wind vector perpendicular to the laser

³Teoste, R., and R. N. Capes, "High-Altitude Infrared Radar Wind Measurements," J Appl Meteorol, 17:1575, 1978.

⁴Schotland, R. M., "The Dual Frequency Doppler Lidar Technique for Wind Measurement," paper presented at the 9th International Laser Radar Conference, Munich, Germany, 1979.

⁵Kunkel, K. E., E. W. Eloranta, and J. A. Weinman, "Remote Determination of Winds, Turbulence Spectra, and Energy Dissipation Rates in the Boundary Layer from Lidar Measurements," J Atmos Sci, 37:978-985, 1980.

⁶Sroga, J. T., E. W. Eloranta, and T. L. Barber, "Lidar Measurement of Wind Velocity Profiles in the Boundary Layer," J Appl Meteorol, Vol 19, No 5, 1980.

⁷Derr, V. E., and C. G. Little, "A Comparison of Remote Sensing of the Clear Atmosphere by Optical, Radio, and Acoustic Radar Techniques," Appl Opt, 9:1976, 1970.

⁸Armstrong, R. L., J. B. Mason, and T. L. Barber, "Detection of Atmospheric Aerosol Flow Using a Transit-Time Lidar Velocimeter," Appl Opt, 15:2891, 1976.

⁹Barber, T. L., and J. B. Mason, "A Transit-Time Lidar Wind Measurement, A Feasibility Study," ECOM-5550, Atmospheric Sciences Laboratory, US Army Electronics Command, White Sands Missile Range, NM, 1974.

beam. Barber and Rodriguez¹⁰ demonstrated the capability of the TTL in extremely clean air conditions. With this technique, the measurement point can be placed at the point of interest, and several measurements along the laser beam can be taken simultaneously. It is quite applicable for ballistic projectile wind correction, because the sampling period is relatively short (10 to 20 s), and the sampling point can be positioned in the path of interest. All of these remote sounding methods depend on tracking the flow of natural dust or haze to measure the wind. This report, however, considers the practicality of using water vapor in a wet atmosphere as a wind tracer. Some of the necessary data handling procedures for this method and for those using dust are similar.

PROCEDURE

This paper considers methods for using variation in absolute water vapor content^{11 12} as a tracer to remotely measure wind speed and wind direction in a wet atmosphere (relative humidity - (RH) high)--where water is essentially in the gas phase. Investigators have remotely measured water vapor content^{11 12} and noted microstructure in the concentration. When a relatively reliable measurement of the water vapor content can be made remotely, the microstructure in the water vapor can be obtained.

Measurement of the microstructure will be done at two well-defined fixed positions in the atmosphere a distance "D" apart (figure 1). Various mathematical techniques can be used to obtain the time for the microstructure to traverse "D." With the distance and time, the wind speed and wind direction perpendicular to the laser beam can be derived.

Two possible techniques for sensing the water vapor content at a point in the atmosphere were considered: (1) ordinary Raman scattering technique¹¹ and (2) DIAL.^{12 13}

Although the ordinary Raman scattering process will produce the necessary information, the inefficiency of this process requires considerable laser power. This necessary power level creates problems for eye safety and equipment size. Investigators using the DIAL technique have found that

¹⁰Barber, T. L., and R. Rodriguez, "Transit-Time Lidar Measurement of Near Surface Winds in the Atmosphere," ASL-TR-0033, US Army Atmospheric Sciences Laboratory, White Sands Missile Range, NM, 1979.

¹¹Cooney, John A., "Comparisons of Water Vapor Profiles Obtained by Radiosonde and Laser Backscatter," J Appl Meteorol, 10:301, 1971.

¹²Schotland, R. M., "Errors in the Lidar Measurement of Atmospheric Gases by Differential Absorption," J Appl Meteorol, 13:71, 1974.

¹³Wright, M. L., et al, "A Preliminary Study of Air Pollution Measurement by Active Remote Sensing Techniques," Final Report, Stanford Research Institute, Menlo Park, CA, 1966.

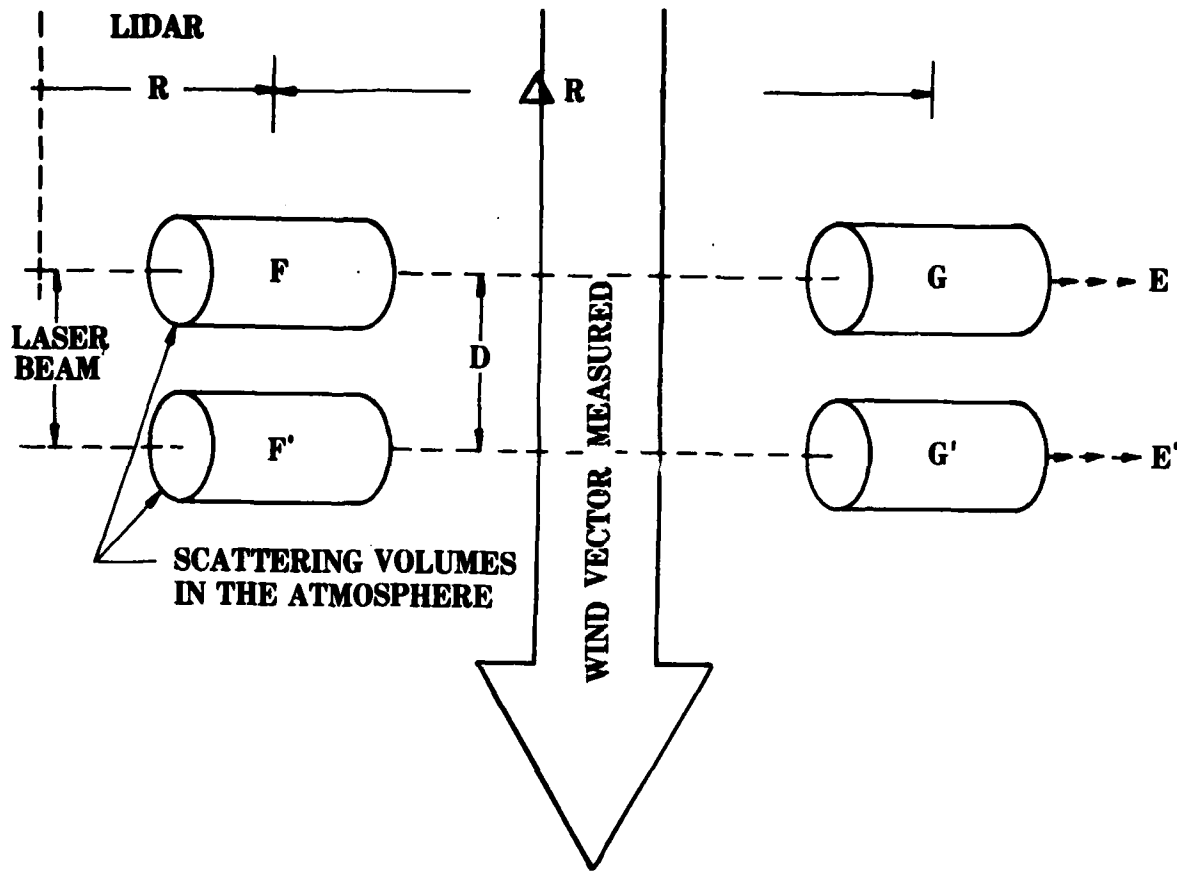


Figure 1. Sample volumes. A graphic portrayal of the scattering volumes in the atmosphere. Both wavelengths A and B will be transmitted along path E. The lidar pointing angle will be changed by some small amount $\Delta\theta$, moving to E'. Wavelengths A and B will be transmitted again along E'. The position along the laser beam can be adjusted by the time delay in the gate circuit. D, the beam spacing, can be calculated by $D = R \sin \Delta\theta$. The total system is shown in figure 2.

measuring water vapor in the atmosphere appears to be the more promising method.^{12 13 14 15 16} This technique involves transmitting two pulsed wavelengths of light along a common path: the first wavelength of light, (A), is essentially not absorbed by water vapor; the other, (B), is appreciably absorbed by water vapor.

Preferably, the wavelength B should be exactly centered on a water vapor absorption line. The lidar receives backscatter from the dust and haze at both wavelengths A and B (figure 1 and figure 2, E) from two common scattering volumes, F and G, making it possible to measure the water vapor content in the volume of interest, ΔR in the interval from F to G. For best results, wavelengths A and B should not be further apart in wavelength than about 0.3 cm^{-1} ,¹² so that the volume backscatter coefficient from the dust and haze in the atmosphere in volumes F and G will essentially be equal. The laser that transmits wavelengths A and B must have a pulse length capable of sufficient range resolution for the approach discussed here, less than 30 ns pulse length. Both wavelengths A and B must be transmitted along the same path in the atmosphere (figure 1, E). These pulses must be no more than a few hundred microseconds from each other⁹ to minimize the problem of changes in atmospheric particulate concentration with time in the scattering volumes. The lidar receives backscattered light from scattering volumes F and G at both wavelengths A and B. These returns will be called P_{AF} and P_{AG} for wavelength A, and P_{BF} and P_{BG} for wavelength B. When transmitting wavelength A, the signal received from the 2 volumes, F and G, will be essentially scatter from the dust and haze affected only by the $1/R^2$ term and scattering losses. R is the range from lidar to scattering volume F. The signal received from the 2 scattering volumes, F and G, will be absorbed by water vapor at wavelength B. Considering one specific beam path (figure 1, E) with a pulse A and a pulse B, four specified scattered returns will be obtained-- P_{AF} , P_{AG} , P_{BF} , and

¹²Schotland, R. M., "Errors in the Lidar Measurement of Atmospheric Gases by Differential Absorption," J Appl Meteorol, 13:71, 1974.

¹³Wright, M. L., et al, "A Preliminary Study of Air Pollution Measurements by Active Remote Sensing Techniques," Final Report, Stanford Research Institute, Menlo Park, CA, 1966.

¹⁴Fraley, P. E., and K. N. Arallal Rao, "High Resolution Infrared Spectra of Water Vapor V, and V₂ Bands of H₂¹⁸O," J Mol Spectroscopy, 29:312-316, 1969.

¹⁵Hinkley, E. D., ed, Laser Monitoring of the Atmosphere, (Berlin, Heidelberg, New York: Springer-Verlag, 1976).

¹⁶Browell, E. V., T. D. Wilkerson, and T. J. McIlrath, "Water Vapor Differential Absorption Lidar Development and Evaluation," Appl Opt, 18:3474, 1979.

⁹Barber T. L., and J. B. Mason, "A Transit-Time Lidar Wind Measurement, A Feasibility Study," ECOM-5550, Atmospheric Sciences Laboratory, US Army Electronics Command, White Sands Missile Range, NM, 1974.

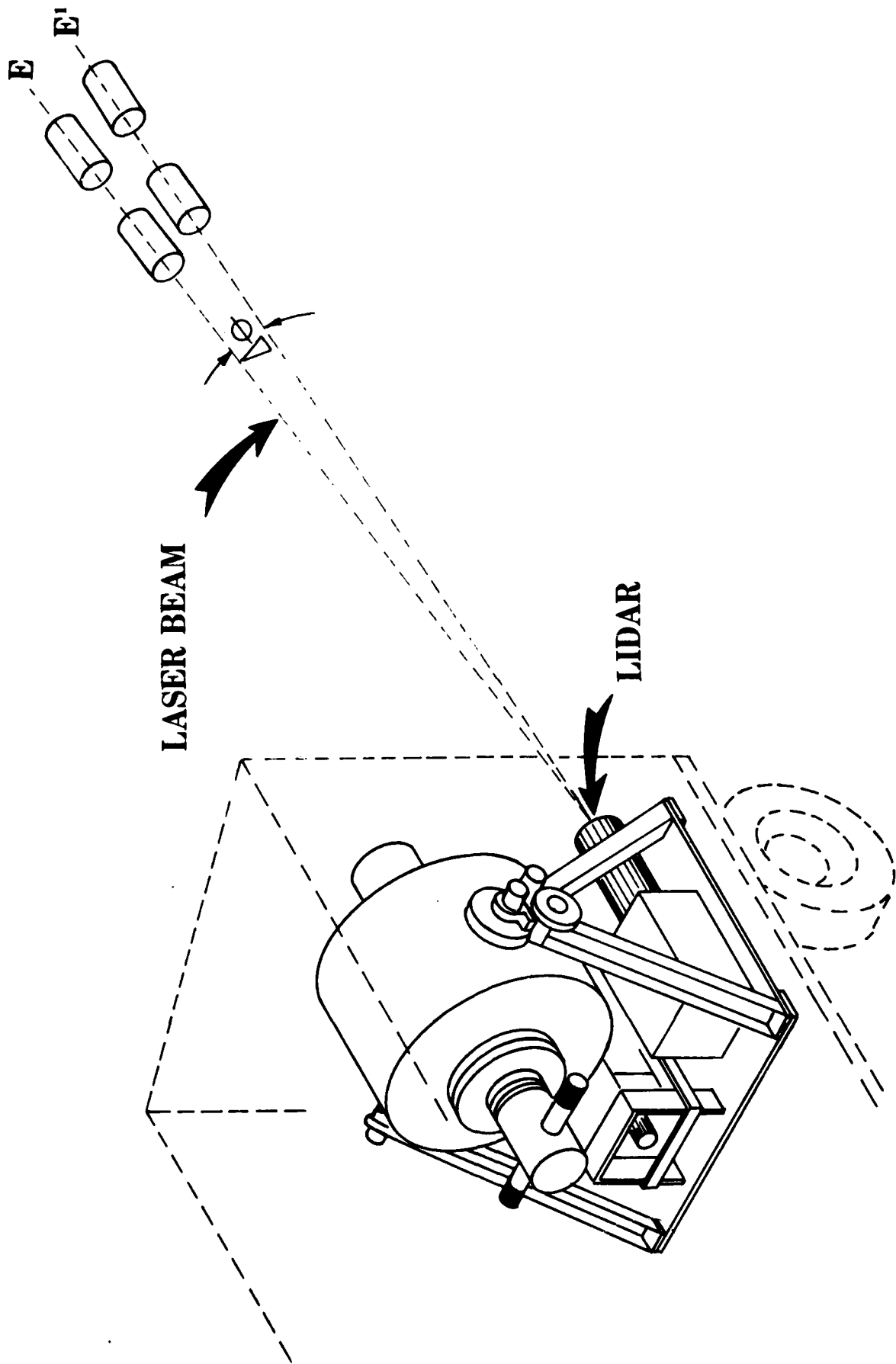


Figure 2. Illustration of total lidar system; laser, receiver and sampling area.

P_{BG} . By using the DIAL technique, a value for the absolute water vapor content in ΔR can be derived.

THEORY

To discuss the fundamentals of remotely measuring the water vapor content, using the DIAL technique, the first step is to consider the fundamental lidar equation:

$$P = P_0 \frac{CT}{2} \beta(R) X R^{-2} \left[\exp -2 \int_0^R \sigma(R) dR \right]. \quad (1)$$

Where P is the received power by the lidar, P_0 is the transmitted power, C is the speed of light, and T is the laser pulse length in time. β is the backscatter coefficient of the atmosphere, X is the effective frontal area of the lidar receiver, and R is the range to the scattering volume of interest. The term $-2 \int_0^R \sigma(R) dR$ gives the extinction along the path R in the atmosphere. σ is the unit volume extinction coefficient in a specific volume of the atmosphere.

The second step is to break down the unit volume extinction coefficient at wavelength B into two parts:

$$\begin{aligned} \sigma_B &= \sigma_S + \sigma_W & (2) \\ \text{and} \\ \sigma_A &= \sigma_S . \end{aligned}$$

Wavelengths A and B have been previously defined. σ_W is the unit volume extinction coefficient at B caused by water vapor absorption. The σ_S is the unit volume extinction coefficient at wavelengths A and B caused by particulate and molecular scattering and minor absorption by materials other than water vapor. This statement concerning σ_S is appropriate since A and B are no further apart in wavelength than 0.3 cm^{-1} .

The third step is to find the relationship between total water vapor and σ_W :

$$\sigma_W = K_W N_W . \quad (3)$$

K_w is the water vapor absorption cross section at wavelength B. N_w is the total water vapor content in 1 unit volume.

Next set:

$$\begin{aligned} C_A &= P_{A0} \frac{CT}{Z} X \\ \text{and} \\ C_B &= P_{B0} \frac{CT}{Z} X \end{aligned} \quad (4)$$

P_{A0} is output power of the lidar at wavelength A, and P_{B0} is the output power of the lidar at B.

With the criteria for A and B as previously stated,

$$\beta_A(R) = \beta_B(R) = \beta(R) \quad (5)$$

Next, two equations are written giving the return at A and B,

$$P_{AF} = C_A \frac{\beta(R)}{R^2} \exp \left[-2 \int_0^R \sigma_S(R) dR \right] \quad (6)$$

$$P_{BF} = C_B \frac{\beta(R)}{R^2} \exp \left\{ -2 \int_0^R [\sigma_S(R) + \sigma_w(R)] dR \right\} \quad (7)$$

The terms $Z(R)$ and $Z(R + DR)$ are now defined as,

$$Z(R) = \ln P_{BF} - \ln P_{AF} \quad \text{and} \quad Z(R + \Delta R) = \ln P_{BG} - \ln P_{AG}$$

and

$$Z(R + DR) = \ln P_{BG} - \ln P_{AG} \quad (8)$$

Inserting (6) and (7) into (8) the resulting two equations are:

$$Z(R) = \ln\left(\frac{C_B}{C_A}\right) - 2 \int_0^R \sigma_w(R) dR ,$$

and

$$Z(R + \Delta R) = \ln\left(\frac{C_B}{C_A}\right) - 2 \int_0^{(R+\Delta R)} \sigma_w(R) dR . \quad (9)$$

If measurements are made at two points (figure 1, F and G), at a range R and range (R + ΔR), to obtain the difference over the length ΔR becomes:

$$Z(R + \Delta R) - Z(R) = -2 \int_R^{R+\Delta R} \sigma_w(R) dR . \quad (10)$$

The $N_{w\Delta R}$ (equation (3)) can be obtained by:

$$\bar{\sigma}_w \Delta R = N_{w\Delta R} K_w = \int_R^{R+\Delta R} \sigma_w(R) dR . \quad (11)$$

The $\bar{\sigma}_w$ is the average value for σ_w over ΔR. Equation (11) becomes:

$$N_{w\Delta R} = \frac{1}{K_w} \int_R^{(R+\Delta R)} \sigma_w(R) dR . \quad (12)$$

$N_{w\Delta R}$ is the total water vapor in the interval ΔR. Rewriting equation 10 results in:

$$Z(R) - Z(R + \Delta R) = 2 \int_R^{(R+\Delta R)} \sigma_w(R) dR \quad (13)$$

or

$$\begin{aligned} \frac{Z(R) - Z(R + \Delta R)}{2} &= \int_R^{(R+\Delta R)} \sigma_w(R) dR \\ &= \bar{\sigma}_w \Delta R \\ &= N_{w\Delta R} K_w \end{aligned} \quad (14)$$

Note that the right portions of equations (11) and (14) are equal. Multiplied by $2/K_w$ equation (14) becomes:

$$\frac{Z(R) - Z(R + \Delta)}{K_w} = 2N_{w\Delta R} \quad (15)$$

Insert the values for $Z(R)$ and $Z(R + \Delta R)$ from equation (8), then

$$N_{w\Delta R} = \frac{1}{2K_w} \left[\ln^P_{BF} - \ln^P_{AF} - \ln^P_{BG} + \ln^P_{AG} \right], \quad (16)$$

or

$$N_{w\Delta R} = \frac{1}{2K_w} \left[\ln \frac{P_{AG}}{P_{AF}} - \ln \frac{P_{BG}}{P_{BF}} \right]. \quad (17)$$

Rearranged, this equation becomes:

$$N_{w\Delta R} = \frac{\bar{\sigma}_w}{K_w} \cdot \Delta R,$$

and

$$N_{w\Delta R} = \bar{\sigma}_w \Delta R .$$

Previously defined, these four values for P are the four signal values measured with a lidar. As formerly stated, the $N_{w\Delta R}$ is the absolute quantity of the water vapor in the interval ΔR . This derivation produces a single value of $N_{w\Delta R}$ for each single set of P_{AF} , P_{AG} , P_{BF} , and P_{BG} .

CALCULATIONS

The previous section gives an outline of the theory related to the DIAL technique. This section will give an example of a wavelength region that can be used for lidar measurements of water vapor. Water vapor has many absorption bands,¹ and the band between 715 and 732 nm is good for water

¹Fraley, P. E., and K. N. Arallal Rao, "High Resolution Infrared Spectra of Water Vapor V, and V₂ Bands of H₂O," J Mol Spectroscopy, 29:312-316, 1969.

vapor measurements.^{16 17} There are 62 absorption lines in this area, carefully measured and described by Wilkerson,¹⁷ that are appropriate to use in the DIAL technique for measuring water vapor. Because the individual line strengths vary through a factor of about 150, different lines can be used in different meteorological conditions. There are also small windows in this region on which to set wavelength A.

The specific example that will be discussed for wavelength B is the line at 723.61 nm. The temperature chosen is 20°C and an RH of 90 percent. The partial pressure at this temperature and RH is 15.79 mm for the water vapor. From Wilkerson et al,¹⁷ the value given for the cross section of water vapor per molecule is $48.2 \cdot 10^{-24} \text{ cm}^2$. With this value and the conditions previously stated, a unit volume extinction due solely to water vapor absorption can be calculated. The number of water molecules in a cubic meter of the atmosphere at this temperature and 1 atmosphere pressure is:

$$\text{no.} = \frac{15.79 \text{ mm}}{760 \text{ mm}} \cdot \frac{273\text{K}}{293\text{K}} \cdot \frac{10^6 / \text{m}^3}{22400 \text{ cm}^3 / \text{mole}} \cdot 6.023 \times 10^{23} = 5.21 \times 10^{23} \text{ molecules.} \quad (18)$$

The cross section per molecule at line center obtained from Wilkerson¹⁷ and multiplied by the number of molecules in the specified volume of interest gives the volume cross section:

$$\sigma_w = 5.21 \times 10^{23} \text{ molecules} \frac{\text{M}^2}{10^6 \text{ cm}^3} \times 48.2 \cdot 10^{-24} \text{ cm}^2 = 2.51 \times 10^{-3} / \text{m} \quad (19)$$

The extinction value $2.51 \times 10^{-3} / \text{m}$ falls well within the values that appear in table 1, column 1, row 5.

Another example that has been worked out in detail in the literature¹⁸ for CO as the molecule and ΔR of 15 m points to the relative accuracy of this approach.

¹⁶Browell, E. V., T. D. Wilkerson, and T. J. McIlrath, "Water Vapor Differential Absorption Lidar Development and Evaluation," Appl Opt, 18:3474, 1979.

¹⁷Wilkerson, T. D., G. Schwemmer, and G. Gentry, "Intensities by N₂ Collision-Broadening Coefficients Measured for Selected H₂O Absorption Lines Between 715 and 732 nm," J Quant Spectroscopy Radiat Transfer, 22:315-331, 1979.

¹⁸Byer, R. L., "Review Remote Air Pollution Measurement," Optical and Quantum Electronics, 7:147-177, 1975.

This case gives an example of the pulse power necessary to achieve the degree of accuracy required in the region of 10 to 100 mJ per pulse.¹⁸ As an example, the range R will be chosen as 490 m and ΔR 10 m. The absolute humidity is the quantity to be measured, so the temperature will be held constant at 20°C. An estimate of the relative data accuracy is shown in this example from the portion inside the large brackets in equation (17).¹⁵ "Given typical detection and digitization equipment, a reasonable value for Δln is about 0.02."¹⁵

Several investigators have examined the types of error that can arise in such a measurement.^{12 15 18 19 20} In the same general type of measurement as discussed here, an absolute accuracy of 1 to 6 percent is shown to be possible.^{18 19} The portion of equation (17) inside the large square bracket can be simplified by considering equation (1). In equation (17), the portion outside the large square brackets (1/2k_w) is a constant for a specific wavelength of B; hence, for a series of measurements where B is not changed, the relative accuracy is not affected. The first term inside the large brackets in equation (17), ln P_{AG}/P_{AF}, can be restated as:

$$\ln \frac{(R + \Delta R)^{-2}}{R^{-2}} \quad (20)$$

The second portion of equation (17) inside large brackets can be rewritten as

$$\ln \frac{(R + \Delta R)^{-2}}{R^{-2}} \cdot \frac{2\sigma_w \Delta R}{1}, \quad (21)$$

or combining the terms inside the large brackets in equation (17):

¹⁸Byer R. L., and Max Garbuny, "Pollutant Detection by Absorption Using Mie Scattering and Topographic Targets as Retroreflectors," Appl Opt, 12:901, 1973.

¹⁵Hinkley E. D., ed, Laser Monitoring of the Atmosphere, (Berlin, Heidelberg, New York: Springer Verlag, 1976).

¹²Schotland, R. M., "Errors in the Lidar Measurement of Atmospheric Gases by Differential Absorption," J Appl Meteorol, 13:71, 1974.

¹⁹Byer, R. L., "Review Remote Air Pollution Measurement," Optical and Quantum Electronics, 7:147-177, 1975.

²⁰Ahmed, Samir A., "Molecular Air Pollution Monitoring by Dye Laser Measurement of Differential Absorption of Atmospheric Elastic Backscatter," Appl Opt, 12:901, 1973.

$$\ln \frac{P_{AG}}{P_{AF}} - \ln \frac{P_{BG}}{P_{BF}} = \ln \frac{(R + \Delta R)^{-2}}{R^{-2}} - \ln \frac{(R + \Delta R)^{-2}}{R^{-2}} \cdot 2\bar{\sigma}_w \Delta R = \Delta \ln = \ln 2\bar{\sigma}_w \Delta R. \quad (22)$$

From a simple examination of equation (17), one can see that the total water vapor content in the interval ΔR is a constant times $\Delta \ln$. For a fixed ΔR , equation (22) shows the dependence of $\bar{\sigma}_w$ in the sample volume on $\Delta \ln$. Equation (17) shows that for a given ΔR the total water vapor content in the interval ΔR is a constant times $\bar{\sigma}_w$. This is the $\bar{\sigma}_w$ measured in ΔR . For best results, keeping a reasonable data quality in this measurement, wavelength B should be chosen so that $\bar{\sigma}_w$ in ΔR will be maintained in a preferred range. In the example considered in table 1, $\Delta R = 10$ m and $R = 490$ m. As previously stated, to maintain a reasonable data quality, physically reasonable value for $\Delta \ln$ is 0.02 or greater. Recall that different values of $\bar{\sigma}_w$ can be attained with a constant water vapor content in the sample volume, by tuning wavelength B to various water vapor absorption lines. Six example water vapor absorption lines are given in table 1. Information in columns 1 and 2 were obtained from Wilkerson.¹⁷ In row 1 of the table, columns 4, 5 and 6 are significantly below 0.02, making this wavelength choice an unfavorable one. At the other extreme, the value in column 3, row 6, presents a different problem. This number is the transmission of wavelength B over a range $2R$. For the case as stated in column 4, row 6, the measurable signal at wavelength B will be reduced by water vapor absorption by a factor of about 23. This reduces the measurement reliability of B. For optimum results, using these two effects as outer bounds, the preferred wavelength chosen should be in the region of rows 2, 3, or 4.

TABLE 1. A COMPARISON OF WATER VAPOR EXTINCTION AND $\Delta \ln$

| | Wavelength B(NM) | $\bar{\sigma}_w$ | | $\Delta \ln$ | | |
|----|---------------------|-------------------|--------|--------------|--------|---------|
| | | $M^{-1} \cdot .1$ | T_0 | RH 65% | RH 90% | RH 115% |
| 1. | 717.59 | 0.0045 | 0.641 | 0.0064 | 0.009 | 0.011 |
| 2. | 717.76 | 0.0109 | 0.336 | 0.015 | 0.021 | 0.027 |
| 3. | 724.08 | 0.0158 | 0.206 | 0.022 | 0.031 | 0.039 |
| 4. | 719.39 | 0.0213 | 0.119 | 0.031 | 0.043 | 0.055 |
| 5. | 723.61 | 0.0251 | 0.0812 | 0.036 | 0.05 | 0.064 |
| 6. | 718.63 | 0.0316 | 0.042 | 0.045 | 0.063 | 0.081 |

¹⁷Wilkerson, T. D., G. Schwemmer, and G. Gentry, "Intensities by N_2 Collision-Broadening Coefficients Measured for Selected H_2O Absorption Lines Between 715 and 732 nm," J Quant Spectroscopy Radiat Transfer, 22:315-331, 1979.

Wavelength is the line center of a specific absorption line for water vapor. σ_w is the extinction in a 1 m path due to water vapor absorption at wavelength B. T_0 is the optical transmission over a path 2R at wavelength B, considering only water vapor absorption. $\Delta \ln$ is described in equation (22).

At this point the question whether sufficient water vapor variation naturally occurs in the atmosphere to make this measurement possible should be considered. Several investigators have measured the high frequency variation of the humidity in the natural atmosphere. Some data have been taken over land surfaces²¹ and rather extensive data at different heights have been taken over the ocean.^{22 23} There is 10 to 15 percent relative variation, compared to the average cell size ranges from 5 to 50 m. This 10 to 15 percent should be adequate to make this wind measuring technique possible.

DATA ANALYSIS

The magnitude of the variations in the water vapor microstructure must be some minimum value or greater to make it practical to measure the wind in this manner. Remember that a portrayal of the water vapor microstructure is produced when a series of single point measurements are taken in a moving medium. With these various results in mind, 10 percent is a reasonable value to require as a minimum in the microstructure variation for a practical measurement. Individuals have observed microstructure in the water vapor by remote sounding.^{11 12} As stated in the last section, fixed point measurements have measured variations approaching 20 percent in the water vapor.

Schotland¹² has made error analyses in several areas of this technique. The change in atmospheric dust with time is a problem. For a single measurement, pulses at wavelength A and B can be no further apart in time than 1 μ s to hold the error to 10 percent. Uncertainties in pressure and temperature in the sampling volume cause an error of approximately 1 percent in the calculated absorption cross section. Schotland performed an error analysis, using a tuneable ruby lidar operating at 694.38 nm, by comparing the water vapor line

²¹Champagne, F. H., C. A. Friehe, and J. C. LaRue, "Flux Measurements, Flux Estimation Techniques, and Fine-Scale Turbulence Measurements in the Unstable Surface Layer Over Land," J Atmos Sci, Vol 34, 1977.

²²Phelps, G. T., and S. Pond, "Spectra of the Temperature and Humidity Fluctuations and of the Fluxes of Moisture and Sensible Heat in the Marine Boundary Layer," J Atmos Sci, Vol 28, 1977.

²³Pond, S., et al, "Measurements of the Turbulent Fluxes of Momentum, Moisture and Sensible Heat Over the Ocean," J Atmos Sci, Vol 34, 1977.

¹¹Cooney, John A., "Comparisons of Water Vapor Profiles Obtained by Radiosonde and Laser Backscatter," J Appl Meteorol, 10:301, 1971.

¹²Schotland, R. M., "Errors in the Lidar Measurement of Atmospheric Gases by Differential Absorption," J Appl Meteorol, 13:71, 1974.

center and laser output for coincidence. The error estimate varied from 3 to 9 percent according to the altitude above sea level where measurements were taken for $\Delta R = 200$ m. With these various results in mind, a reasonable value to require as a minimum in the microstructure variation is 20 percent for a practical measurement. Schotland (personal communication, 1981), using a DIAL system to measure water vapor, estimated a microstructure variation of at least 10 percent over noise. Cooney (personal communication, 1981), using a Raman lidar, had observed microstructure variations of about 25 percent in the water vapor content. In cases such as these, it is possible to use the water vapor variation as a tracer to remotely measure wind velocity.

To use variations in water vapor content in the atmosphere to measure a component of the wind velocity remotely perpendicular to the lidar beam, the water vapor variation must be tracked. A method for doing this tracking in a moving medium--the wind moving the atmosphere--can be done by measuring the microstructure at two fixed positions a known distance apart. The time of flight, then, can be determined across these two positions. This is done by first taking a set of single measurements at a known rate at 2 fixed points in space. By plotting the relative magnitude of these values, a portrayal of the water vapor microstructure can be obtained.

The time of flight is obtained by cross-correlating these two sets of data, hence deriving a time ΔT , over the distance D . The wind velocity, on a line through the center of these two points, is $(D/\Delta T) = VD$. Several parameters must be considered carefully before taking a meaningful data set, so that the necessary information to derive the wind velocity is available. The first question asked is how many individual samples per second should be taken for good results. This has been discussed previously⁹ ¹⁰ for tracking natural atmospheric dust. A sampling rate adequate for this purpose is 1000 samples per second. When these values are collected, the group or data block from one scattering volume should be broken down into smaller groups: for example, 25 individual values. These values should be averaged with each of the average values grouped as a second data block reducing occasional sharp irregularities in such data. These irregularities¹⁰ are felt to be caused by optical turbulence in the laser beam, from lidar to sample volume. With these 2 new blocks of average data points, one from each of the 2 fixed positions, the next step to consider is how much total time the block should cover. Here it might be imagined that the longer the total period, the easier to determine ΔT . This is not the case because the wind is a constantly changing parameter. Considering this, along with past experience in similar lidar techniques, a total time of about 10 s is reasonable. If during this period of time, however, the wind velocity changes radically when the two data blocks are cross-correlated, this change substantially degrades the cross-correlation results.

⁹Barber T. L., and J. B. Mason, "A Transit-Time Lidar Wind Measurement, A Feasibility Study," ECOM-5550, Atmospheric Sciences Laboratory, US Army Electronics and Development Command, White Sands Missile Range, NM, 1979.

¹⁰Barber T. L., and R. Rodriguez, "Transit-Time Lidar Measurement of Near Surface Winds in the Atmosphere," ASL-TR-0033, US Army Atmospheric Sciences Laboratory, White Sands Missile Range, NM, 1979.

Another consideration in this methodology is the value for D (figure 1). There are two limits. If D is too small, for example 1 m, this limits the higher wind velocities that can be measured. With the previously stated average value rate $25/1000 = 1/40$ s, the two highest wind values that are measurable are 40 m/s and 20 m/s.

If a value for D is too large, for example 300 m, the microstructure can change appreciably from one volume to the next. "D" should occur in the range 5 to 15 m, generally the same as ΔR . The total number of points that most computer systems will accept in the cross-correlation procedure adds further difficulty in this area. This procedure generally is 4096 points in each of the two averaged blocks. For each averaged point in the example given above, $1/40$ s period is covered or 40/s. In 10 s of time, this will be 400 values.

In most cross-correlation procedures, 512 points can be used. Recall that all the previous numbers given--the sampling rate, 1000 per s, the quantity averaged 25, and the total time of the sample 10 s--are all given to identify a region, not a specific number. These numbers can all be adjusted to permit 512 data points to be obtained. Here, the two blocks of data are available with the information of the water vapor microstructure necessary for deriving wind velocity value.

Focusing the processing on the information of interest in the data is the next point to be considered. This focusing is done by frequency filtering the two averaged data blocks. To obtain an indication of the frequency components of interest, an example will be used with a 10 m/s wind. The highest frequency in the data is caused by the small irregularity passing through a sample volume. As an example, a 4-m irregularity moving along in the wind will cause 2.5 Hz components in the data. The 4-m size is about the smallest change that should be considered. This comes about because of the 10 m ΔR . Little more than 1 irregularity at a time can occur in the sample volume. The 4-m variation moving along in a 10-m wind will pass through the sampling point in 0.04 s, hence 2.5 Hz. As in the next case, a 10-m irregularity in the water vapor microstructure will take 1 s to pass through one volume, hence 1 Hz. As the irregularity being considered gets larger, for example up to 100 m in extent, the frequency component in the data becomes 0.01 Hz. With this wind velocity, it would pass through one volume in 10 s--the total period of the sample. One complete cycle of this frequency in the data is of little value. A good point at which to set the low frequency cut-off is 0.02Hz. When these two data blocks have been properly filtered, they are cross-correlated to produce ΔT . When ΔT is obtained, the wind velocity is $D/\Delta T = V$. V is the wind velocity component on a line through the two sampling volumes.

High RH conditions will probably be a more reliable measurement than using dust and haze as the tracer,^{9 10} but with this technique, information to

⁹Barber T. L., and J. B. Mason, "A Transit-Time Lidar Wind Measurement, A Feasibility Study," ECOM-5550, Atmospheric Sciences Laboratory, US Army Electronics Command, White Sands Missile Range, NM, 1974.

¹⁰Barber T. L., and R. Rodriguez, "Transit-Time Lidar Measurement of Near Surface Winds in the Atmosphere," ASL-TR-0033, US Army Atmospheric Sciences Laboratory, White Sands Missile Range, NM, 1979.

derive a wind velocity by tracking dust and haze irregularities is available. Remember that using P_{AF} and P_{AG} provides the necessary information¹⁰ to derive the wind velocity from tracking natural dust and haze.

CONCLUSIONS

The feasibility for using the natural water vapor microstructure as a tracer for remote wind measurements in a wet atmosphere was shown. This microstructure tracking is felt to be a most appropriate technique for meteorological conditions where high RH is prevalent.

Of interest here is the relative variation in the absolute water vapor content of the atmosphere. The variations or microstructures are measured at two fixed points a known distance apart. The wind velocity can be derived by determining the time of flight from one measuring position to the other.

For these procedures to produce the information of interest, the DIAL measurements of the absolute water vapor content must be taken with some care regarding the water vapor extinction coefficient in ΔR sampling rate, sampling period, and data frequency filtering.

When an initial set of water vapor data is collected, filtering should be done carefully to focus the tracking process on water vapor irregularities in a general size range 4 to 100 m. When the processing is aimed toward tracking a general size of irregularity, a reasonable cross correlation is available; hence, the wind velocity can be derived.

This technique has the potential of working quite well in certain meteorological conditions. Recall that in this same data, information is available to implement use of water vapor or to implement use of dust and haze as the tracer. The combination is certainly much more reliable in a wider variety of meteorological conditions than either method alone.

The percentage of time that adequate conditions occur in the water vapor microstructure to allow a reasonable wind measurement is an area that should be investigated further.

⁹Barber, T. L., and J. B. Mason, "A Transit-Time Lidar Wind Measurement, A Feasibility Study," ECOM-5550, Atmospheric Sciences Laboratory, US Army Electronics Command, White Sands Missile Range, NM, 1974.

¹⁰Barber, T. L., and R. Rodriguez, "Transit-Time Lidar Measurement of Near Surface Winds in the Atmosphere," ASL-TR-0033, US Army Atmospheric Sciences Laboratory, White Sands Missile Range, NM, 1979.

REFERENCES

1. Schwiesow, R. L., and R. E. Cupp, "Remote Doppler Velocity Measurements of Atmospheric Dust Devil Varieties," Appl Opt, 15:1, 1976.
2. Post, M. J., et al, "A Comparison of Anemometer and Lidar Sensed Wind Velocity Data," J Appl Meteorol, 17:1179-1181, 1978.
3. Teoste, R., and R. N. Capes, "High-Altitude Infrared Radar Wind Measurements," J Appl Meteorol, 17:1575, 1978.
4. Schotland, R. M., "The Dual Frequency Doppler Lidar Technique for Wind Measurement," paper presented at the 9th International Laser Radar Conference, Munich, Germany, 1979.
5. Kunkel, K. E., E. W. Eloranta, and J. A. Weinman, "Remote Determination of Winds, Turbulence Spectra, and Energy Dissipation Rates in the Boundary Layer from Lidar Measurements," J Atmospheric Sci, 37:978-985, 1980.
6. Sroga, J. T., E. W. Eloranta, and T. L. Barber, "Lidar Measurement of Wind Velocity Profiles in the Boundary Layer" accepted for publication J Appl Meteorol, Vol 19, No 5, 1980.
7. Derr, V. E., and C. G. Little, "A Comparison of Remote Sensing of the Clear Atmosphere by Optical, Radio, and Acoustic Radar Techniques," Appl Opt, 9:1976, 1970.
8. Armstrong, R. L., J. B. Mason, and T. L. Barber, "Detection of Atmospheric Aerosol Flow Using a Transit-Time Lidar Velocimeter," Appl Opt, 15:2891, 1976.
9. Barber, T. L., and J. B. Mason, "A Transit-Time Lidar Wind Measurement, A Feasibility Study," ECOM-5550, Atmospheric Sciences Laboratory, US Army Electronics Command, White Sands Missile Range, NM, 1974.
10. Barber, T. L., and R. Rodriguez, "Transit-Time Lidar Measurement of Near Surface Winds in the Atmosphere," ASL-TR-0033, US Army Atmospheric Sciences Laboratory, White Sands Missile Range, NM, 1979.
11. Cooney, John A., "Comparisons of Water Vapor Profiles Obtained by Radiosonde and Laser Backscatter," J Appl Meteorol, 10:301, 1971.
12. Schotland, R. M., "Errors in the Lidar Measurement of Atmospheric Gases by Differential Absorption," J Appl Meteorol, 13:71, 1974.
13. Wright, M. L. et al, "A Preliminary Study of Air Pollution Measurement by Active Remote Sensing Techniques," Final Report, Stanford Research Institute, Menlo Park, CA, 1966.
14. Fraley, P. E., and K. N. Arallal Rao, "High Resolution Infrared Spectra of Water Vapor V, and V₂ Bands of H₂O," J Mol Spectroscopy, 29:312-316, 1969.
15. Hinkley, E. D., ed, Laser Monitoring of the Atmosphere, (Berlin, Heidelberg, New York: Springer-Verlag, 1976).

16. Browell, E. V., T. D. Wilkerson, and T. J. McIlrath, "Water Vapor Differential Absorption Lidar Development and Evaluation," Appl Opt, 18:3474, 1979.
17. Wilkerson, T. D., G. Schwemmer, and G. Gentry, 1979, "Intensities by N₂ Collision-Broadening Coefficients Measured for Selected H₂O Absorption Lines Between 715 and 732 nm," J Quant Spectroscopy Radiat Transfer, 22:315-331, 1979.
18. Byer, Robert L., and Max Garbuny, "Pollutant Detection by Absorption Using Mie Scattering and Topographic Targets as Retroreflectors," Appl Opt, 12:901, 1973.
19. Byer, R. L., "Review Remote Air Pollution Measurement," Optical and Quantum Electronics, 7:147-177, -1975.
20. Ahmed, Samir A., "Molecular Air Pollution Monitoring by Dye Laser Measurement of Differential Absorption of Atmospheric Elastic Backscatter," Appl Opt, 12:901, 1973.
21. Champagne, F. H., C. A. Friehe, and J. C. LaRue, "Flux Measurements, Flux Estimation Techniques, and Fine-Scale Turbulence Measurements in the Unstable Surface Layer Over Land," J Atmos Sci, Vol 34, 1977.
22. Phelps, G. T., and S. Pond, "Spectra of the Temperature and Humidity Fluctuations and of the Fluxes of Moisture and Sensible Heat in the Marine Boundary Layer," J Atmos Sci, Vol 28, 1977.
23. Pond, S., et al, "Measurements of the Turbulent Fluxes of Momentum, Moisture and Sensible Heat Over the Ocean," J Atmos Sci, Vol 34, 1977.

DISTRIBUTION LIST

Commander
US Army Aviation Center
ATTN: ATZQ-D-MA
Fort Rucker, AL 36362

John M. Hobbie
c/o Kentron International
2003 Byrd Spring Road
Huntsville, AL 35807

Chief, Atmospheric Sciences Div
Code ES-81
NASA
Marshall Space Flight Center, AL 35812

Commander
US Army Missile Command
ATTN: DRDMI-RRA/Dr. O. M. Essenwanger
Redstone Arsenal, AL 35809

Commander
US Army Missile Command
ATTN: DRSMI-OG (B. W. Fowler)
Redstone Arsenal, AL 35809

Commander
US Army Missile R&D Command
ATTN: DRDMI-TEM (R. Haraway)
Redstone Arsenal, AL 35809

Redstone Scientific Information Center
ATTN: DRSMI-RPRD (Documents)
US Army Missile Command
Redstone Arsenal, AL 35809

Commander
HQ, Fort Huachuca
ATTN: Tech Ref Div
Fort Huachuca, AZ 85613

Commander
US Army Intelligence
Center & School
ATTN: ATSI-CD-MD
Fort Huachuca, AZ 85613

Commander
US Army Yuma Proving Ground
ATTN: Technical Library
Bldg 2105
Yuma, AZ 85364

Dr. Frank D. Eaton
Geophysical Institute
University of Alaska
Fairbanks, AK 99701

Naval Weapons Center
Code 3918
ATTN: Dr. A. Shlanta
China Lake, CA 93555

Commanding Officer
Naval Envir Prediction Rsch Facility
ATTN: Library
Monterey, CA 93940

Sylvania Elec Sys Western Div
ATTN: Technical Reports Lib
PO Box 205
Mountain View, CA 94040

Tetra Tech Inc.
ATTN: L. Baboolal
630 N. Rosemead Blvd.
Pasadena, CA 91107

Geophysics Officer
PMTC Code 3250
Pacific Missile Test Center
Point Mugu, CA 93042

Commander
Naval Ocean Systems Center
(Code 4473)
ATTN: Technical Library
San Diego, CA 92152

Meteorologist in Charge
Kwajalein Missile Range
PO Box 67
APO San Francisco, CA 96555

Director
NOAA/ERL/APCL R31
RB3-Room 567
Boulder, CO 80302

Library-R-51-Tech Reports
NOAA/ERL
320 S. Broadway
Boulder, CO 80303

National Center for Atmos Rsch
Mesa Library
P. O. Box 3000
Boulder, CO 80307

Dr. B. A. Silverman D-1200
Office of Atmos Resources Management
Water and Power Resources Service
PO Box 25007
Denver Federal Center, Bldg. 67
Denver, CO 80225

Hugh W. Albers (Executive Secretary)
CAO Subcommittee on Atmos Rsch
National Science Foundation Room 510
Washington, DC 2055

Dr. Eugene W. Bierly
Director, Division of Atmos Sciences
National Science Foundation
1800 G Street, N.W.
Washington, DC 20550

Commanding Officer
Naval Research Laboratory
Code 2627
Washington, DC 20375

Defense Communications Agency
Technical Library Center
Code 222
Washington, DC 20305

Director
Naval Research Laboratory
Code 5530
Washington, DC 20375

Dr. J. M. MacCallum
Naval Research Laboratory
Code 1409
Washington, DC 20375

HQDA (DAMI-ISP/H. Tax)
Washington, DC 20314

HQDA (DAEN-RDM/Dr. de Percin)
Washington, DC 20314

The Library of Congress
ATTN: Exchange & Gift Div
Washington, DC 20540

2

Mil Asst for Atmos Sci Ofc of
the Undersecretary of Defense
for Rsch & Engr/E&LS - RM 3D129
The Pentagon
Washington, DC 20301

Dr. John L. Walsh
Code 6534
Navy Research Lab
Washington, DC 20375

AFATL/DLODL
Technical Library
Eglin AFB, FL 32542

Naval Training Equipment Center
ATTN: Technical Information Center
Orlando, FL 32813

Technical Library
Chemical Systems Laboratory
Aberdeen Proving Ground, MD 21010

US Army Materiel Systems
Analysis Activity
ATTN: DRXSY-MP
APG, MD 21005

Commander
ERADCOM
ATTN: DRDEL-PA/ILS/-ED
2800 Powder Mill Road
Adelphi, MD 20783

Commander
ERADCOM
ATTN: DRDEL-PAO (M. Singleton)
2800 Powder Mill Road
Adelphi, MD 20783

Commander
ERADCOM
ATTN: DRDEL-ST-T (Dr. B. Zarwyn)
2800 Powder Mill Road
Adelphi, MD 20783
02

Commander
Harry Diamond Laboratories
ATTN: DELHD-CO
2800 Powder Mill Road
Adelphi, MD 20783

Chief
Intel Mat Dev & Spt Ofc
ATTN: DELEW-WL-I
Bldg 4554
Fort George G. Mead, MD 20755

Acquisitions Section, IRDB-D823
Library & Info Svc Div, NOAA
6009 Executive Blvd.
Rockville, MD 20752

Naval Surface Weapons Center
White Oak Library
Silver Spring, MD 20910

Air Force Geophysics Laboratory
ATTN: LCC (A. S. Carten, Jr.)
Hanscom AFB, MA 01731

Air Force Geophysics Laboratory
ATTN: LYD
Hanscom AFB, MA 01731

Meteorology Division
AFGL/LY
Hanscom AFB, MA 01731

The Environmental Research
Institute of MI
ATTN: IRIA Library
PO Box 8618
Ann Arbor, MI 48107

Mr. William A. Main
USDA Forest Service
1407 S. Harrison Road
East Lansing, MI 48823

Dr. A. D. Belmont
Research Division
PO Box 1249
Control Data Corp
Minneapolis, MN 55440

Commander
Naval Oceanography Command
Bay St. Louis, MS 39529

Commanding Officer
US Army Armament R&D Command
ATTN; DRDAR-TSS Bldg 59
Dover, NJ 07801

Commander
ERADCOM Scientific Advisor
ATTN: DRDEL-SA
Fort Monmouth, NJ 07703

Commander
ERADCOM Tech Support Activity
ATTN: DELSD-L
Fort Monmouth, NJ 07703

Commander
HQ, US Army Avionics R&D Actv
ATTN: DAVAA-O
Fort Monmouth, NJ 07703

Commander
USA Elect Warfare Lab
ATTN: DELEW-DA (File Cy)
Fort Monmouth, NJ 07703

Commander
US Army Electronics R&D Command
ATTN: DELCS-S
Fort Monmouth, NJ 07703

Commander
US Army Satellite Comm Agency
ATTN: DRCPM-SC-3
Fort Monmouth, NJ 07703

Commander/Director
US Army Combat Survl & Target
Acquisition Laboratory
ATTN: DELCS-D
Fort Monmouth, NJ 07703

Director
Night Vision & Electro-Optics Laboratory
ATTN: DELNV-L (Dr. R. Buser)
Fort Belvoir, VA 22060

Project Manager
FIREFINDER/REMBASS
ATTN: DRCPM-FFR-TM
Fort Monmouth, NJ 07703

6585 TG/WE
Holloman AFB, NM 88330

AFWL/Technical Library (SUL)
Kirtland AFB, NM 87117

AFWL/WE
Kirtland, AFB, NM 87117

TRASANA
ATTN: ATAA-SL (D. Anguiano)
WSMR, NM 88002

Commander
US Army White Sands Missile Range
ATTN: STEWS-PT-AL
White Sands Missile Range, NM 88002

Rome Air Development Center
ATTN: Documents Library
TSLD (Bette Smith)
Griffiss AFB, NY 13441

Environmental Protection Agency
Meteorology Laboratory, MD 80
Rsch Triangle Park, NC 27711

US Army Research Office
ATTN: DRXRO-PP
PO Box 12211
Rsch Triangle Park, NC 27709

Commandant
US Army Field Artillery School
ATTN: ATSF-CD-MS (Mr. Farmer)
Fort Sill, OK 73503

Commandant
US Army Field Artillery School
ATTN: ATSF-CF-R
Fort Sill, OK 73503

Commandant
US Army Field Artillery School
ATTN: Morris Swett Library
Fort Sill, OK 73503

Commander
US Army Dugway Proving Ground
ATTN: STEDP-MT-DA-M
(Mr. Paul Carlson)
Dugway, UT 84022

Commander
US Army Dugway Proving Ground
ATTN: MT-DA-L
Dugway, UT 84022

US Army Dugway Proving Ground
ATTN: STEDP-MT-DA-T
(Dr. W. A. Peterson)
Dugway, UT 84022

Inge Dirmhirm, Professor
Utah State University, UMC 48
Logan, UT 84322

Defense Technical Information Center
ATTN: DTIC-DDA-2
Cameron Station, Bldg. 5
Alexandria, VA 22314
12

Commanding Officer
US Army Foreign Sci & Tech Cen
ATTN: DRXST-IS1
220 7th Street, NE
Charlottesville, VA 22901

Naval Surface Weapons Center
Code G65
Dahlgren, VA 22448

Commander
US Army Night Vision
& Electro-Optics Lab
ATTN: DELNV-D
Fort Belvoir, VA 22060

Commander
USATRADO
ATTN: ATCD-FA
Fort Monroe, VA 23651

Commander
USATRADO
ATTN: ATCD-IR
Fort Monroe, VA 23651

Dept of the Air Force
5WW/DN
Langley AFB, VA 23665

US Army Nuclear & Cml Agency
ATTN: MONA-WE
Springfield, VA 22150

Director
US Army Signals Warfare Lab
ATTN: DELSW-OS (Dr. Burkhardt)
Vint Hill Farms Station
Warrenton, VA 22186

Commander
US Army Cold Regions Test Cen
ATTN: STECR-OP-PM
APO Seattle, WA 98733

END

A

FILMED

1-83

DTIC